In situ Near-Ambient Pressure X-ray Photoelectron Spectroscopy Reveals the Influence of Photon Flux and Water on the Stability of Halide Perovskite

M. Kot,*[a, b] L. Kegelmann,[c] H. Köbler,[c] M. Vorokhta,[d] C. Escudero,[e] P. Kúš,[d] B. Šmíd,[d] M. Tallarida,[e] S. Albrecht,[c] A. Abate,[c] I. Matolínová,[d] D. Schmeißer,[a] and J. I. Flege[b]

For several years, scientists have been trying to understand the mechanisms that reduce the long-term stability of perovskite solar cells. In this work, we examined the effect of water and photon flux on the stability of $CH_3NH_3PbI_3$ perovskite films and solar cells using in situ near-ambient pressure X-ray photoelectron spectroscopy (NAP-XPS), field emission scanning electron microscopy (FESEM), and current density–voltage (*J–V*) characterization. The used amount of water vapor (up to 1 mbar) had a negligible impact on the perovskite film. The higher the photon flux, the more prominent were the changes in the NAP-XPS and FESEM data; also, a faster decline in power conversion efficiency (PCE) and a more substantial hysteresis in the *J-V* characteristics were observed. Based on our results, it can be concluded that the PCE decrease originates from the creation of Frenkel pair defects in the perovskite film under illumination. The stronger the illumination, the higher the number of Frenkel defects, leading to a faster PCE decline and more substantial hysteresis in the *J-V* sweeps.

1. Introduction

After several years of efficiency-driven research on perovskite solar cells (PSCs),[1–4] the focus is now shifting to understand the underlying processes governing the high efficiency and also to obtain long-term stable devices.[5–7] It has been shown that PSCs degrade under outdoor conditions such as humidity, oxygen, temperature, UV light, intense light irradiation, and also when applying electric fields.[8–10] In particular, the instability of PSCs is widely conceived to be humidity-induced due to the water solubility of its initial precursors. However, it was also reported that the perovskite films by themselves could withstand humidity, and it is instead the photon flux that leads to device degradation or the photon flux in combination with humidity exposure.[11] Moreover, it was also claimed that PSCs degrade due to the reactive TiO_2/perovskite interface and due to the surface defects of the TiO_2,[12,13] which are activated with light and result in an imbalance of charges in the perovskite crystals. Besides that, by combining light and humid air the internal luminescence quantum efficiencies of polycrystalline perovskite films was improved.[14] In particular, the photoluminescence studies have shown that illumination of perovskite films reduces trap density in dependence on the light dose[15] that can be boosted further in the presence of oxygen.[16] Thus, increasing and controlling the perovskite stability, along with understanding the main degradation pathways, is a crucial issue for the development of commercially viable devices.

In this work, to assess the influence of water, photons, and TiO_2 on the perovskite films' stability, we monitored the photon and water interaction with $CH_3NH_3PbI_3$ (MAPI) films prepared directly on fluorine-doped tin oxide (FTO) substrates (no TiO_2) in situ by conducting near-ambient pressure X-ray photoelectron spectroscopy (NAP-XPS). NAP-XPS experiments were performed using both laboratory- and synchrotron-based instruments, providing comparatively lower photon flux and significantly higher and adjustable photon flux, respectively. The effect of the different treatments in the NAP-XPS systems on the perovskite surface morphology was investigated by field emission scanning electron microscopy (FESEM). The influence of illumination on the PSCs' performance and long-term stability was investigated by conducting repeated current density–voltage (*J-V*) scans under varied lighting. Our results indicate that the used amount of water has a much lower impact on the PSCs degradation than the applied photon flux during the experiments, that is, the higher the photon flux, the faster the perovskite degradation.

[a] *Dr. M. Kot, Prof. D. Schmeißer*
Applied Physics and Sensors
Brandenburg University of Technology Cottbus-Senftenberg
Konrad-Wachsmann-Allee 17, 03046 Cottbus (Germany)
E-mail: malgorzata.sowinska@b-tu.de
[b] *Dr. M. Kot, Prof. J. I. Flege*
Applied Physics and Semiconductor Spectroscopy
Brandenburg University of Technology Cottbus-Senftenberg
Konrad-Zuse-Strasse 1, 03046 Cottbus (Germany)
[c] *Dr. L. Kegelmann, H. Köbler, Prof. S. Albrecht, Prof. A. Abate*
Helmholtz-Zentrum Berlin für Materialien und Energie GmbH
Kekuléstrasse 5, 12489 Berlin (Germany)
[d] *Dr. M. Vorokhta, Dr. P. Kúš, Dr. B. Šmíd, Prof. I. Matolínová*
Charles University, Faculty of Mathematics and Physics
Department of Surface and Plasma Science
V Holešovičkách 2, 18000 Prague 8 (Czech Republic)
[e] *Dr. C. Escudero, Dr. M. Tallarida*
ALBA Synchrotron
Carrer de la Llum 2–26, 08290 Cerdanyola del Vallès (Spain)

Supporting information for this article is available on the WWW under https://doi.org/10.1002/cssc.202001527

© 2020 The Authors. Published by Wiley-VCH GmbH. This is an open access article under the terms of the Creative Commons Attribution Non-Commercial NoDerivs License, which permits use and distribution in any medium, provided the original work is properly cited, the use is non-commercial and no modifications or adaptations are made.

Interestingly, the light-induced degradation of the MAPI films occurred even in the absence of the TiO_2 layer underneath. In ageing tests of corresponding solar cells, initially, a steep drop in power conversion efficiency (PCE) was observed, which depended on the used photon flux. By comparing the ageing *J–V* with in situ NAP-XPS and FESEM studies, we attribute this effect to the photon-induced decomposition and creation of Frenkel defects in the perovskite crystal.

2. Results

Initially, the $CH_3NH_3PbI_3$/FTO/glass sample was subjected to different water vapor pressures in the laboratory-based NAP-XPS system[17,18] and investigated in situ employing a monochromatized Al K_α X-ray source with excitation energy of 1486.6 eV in a normal emission geometry. The photon flux was equal to 6.1×10^9 photons s^{-1}, and it is the lowest used in this work during the NAP-XPS studies. In Figure 1, the C 1*s* (a), N 1*s* (b), Pb 4*f* (c), I 4*d* (d), valence band (VB, e), and O 1*s* (f) spectra were taken on the $CH_3NH_3PbI_3$ surface being exposed to ultra-high vacuum (UHV; $\approx1\times10^{-9}$ mbar) and 10^{-3}, 10^{-2}, 10^{-1}, and 1 mbar of water vapor. The sample was investigated twice under UHV conditions: a first time before (UHV_{start}) and a second time after (UHV_{end}) exposition to water vapor. It should be noted that these XPS spectra were collected on the same spot of the MAPI film, that is, the "1 mbar" spectrum was obtained after continuously exposing the MAPI film to the X-rays (and water vapor) for 9.5 h. The last spectrum taken in the same spot on the MAPI film was again collected after pumping down the system to UHV (UHV_{end}) conditions. Additionally, the NAP-XPS spectra were obtained under UHV conditions at another spot of the same MAPI sample previously being exposed to water ($UHV_{end\ fresh\ spot}$ in Figure 1).

The as-prepared MAPI film [measured in UHV without any water insertion (UHV_{start})] shows two components in the C 1*s* peak (Figure 1a), one located at 285.3 eV and one at 286.6 eV. The lower binding energy (BE) component can be attributed to hydrocarbon[19] or CH_3I[20] and the other component to C–N bonding in the methylammonium.[19] In the N 1*s* level (Figure 1b) only one peak is detected at a BE of 402.6 eV, typical for nitrogen bonding in the MAPI film.[6,18] In the Pb 4*f* spectrum (Figure 1c) only a doublet peak related to the MAPI film with the Pb $4f_{7/2}$ position at 138.6 eV is observed, in agreement with previous studies.[6,21] No additional peak at 136.8 eV that could be related to "metallic Pb"[22] is found. For the I 4*d* peak (Figure 1d), the BE of the 5/2 level is equal to 49.6 eV indicating a bonding between the organic molecule and iodine.[23] The valence band maximum (VBM, Figure 1e) is located around 1.47 eV below the Fermi level. Having in mind the reported optical band gap of 1.56 eV[24] of the MAPI film, the Fermi level position being closer to the conduction band minimum indicates an n-type character[21] of the investigated film at its surface. The sample also contained a minimal amount of oxygen. The O 1*s* peak was located at the binding energy of 532.8 eV. It could arise from the adsorption of OH groups during sample transfer to the NAP-XPS system in the air or from the solvents' residuals[6] during the film preparation. When the as-prepared MAPI film was then continuously exposed to water vapor and X-rays, a decrease of the higher BE peak (286.6 eV, CH_3NH_3) in the C 1*s* and the N 1*s* peak (402.6 eV, CH_3NH_3) is visible in the NAP-XPS spectra. No peak shifts or the appearance of new components are observed. Besides the nitrogen and carbon reduction, the amount of iodine and lead in the MAPI subsurface region (considering a probing depth of the XPS method using Al K_α radiation source and normal emission geometry of up to approximately 10 nm) increased. When increasing the water vapor pressure in the NAP-XPS chamber, a peak at 535.8 eV appears in the O 1*s* XPS spectra that corresponds to the typical footprint of water in the gas phase. As soon as the system was pumped down to UHV conditions again, the peak at 535.8 eV disappeared completely (UHV_{end}). If the experiment had been concluded at this stage, the conclusion would have been that water irreversibly destroyed

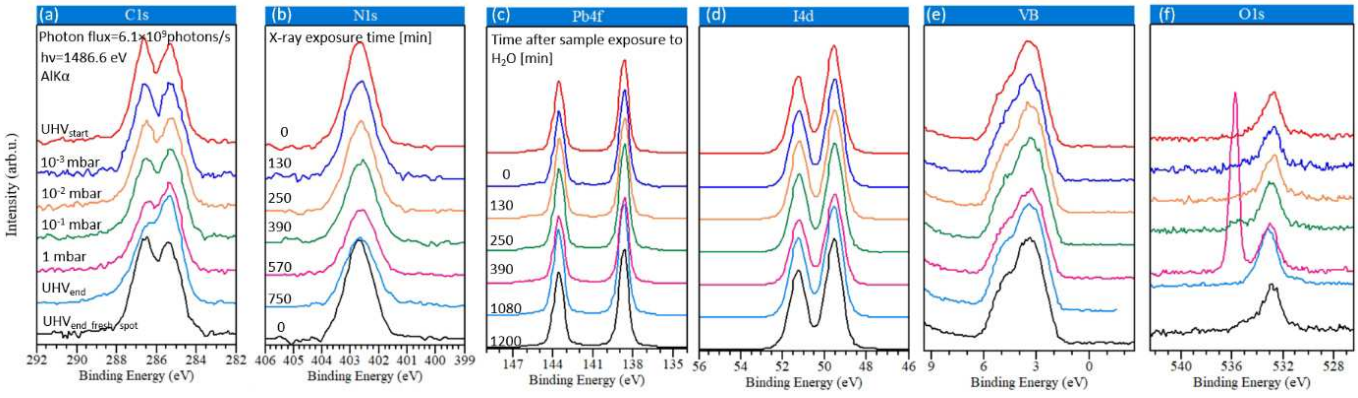

Figure 1. Exposure of the $CH_3NH_3PbI_3$ to the laboratory-based X-rays (lowest used photon flux of 6.1×10^9 photon s^{-1}, 0.01 sun) and water vapor. C 1*s* (a), N 1*s* (b), Pb 4*f* (c), I 4*d* (d), VB (e) and O 1*s* (f) NAP-XPS spectra of the $CH_3NH_3PbI_3$ film prepared on the FTO/glass substrate and exposed to different water vapor pressures using an excitation energy of 1486.6 eV (Al K_α radiation). In the experiment the as-prepared sample (UHV_{start}), exposed to 10^{-3}, 10^{-2}, 10^{-1}, and 1 mbar of water vapor and measured again in the UHV conditions (UHV_{end}) was investigated in the same spot on the sample. Additionally, $CH_3NH_3PbI_3$ film after exposition to water vapor was investigated again on the fresh spot ($UHV_{end\ fresh\ spot}$). The initial time of the sample exposure to X-rays and the time after sample exposure to water vapor are indicated in (b) and (c), respectively.

© 2020 The Authors. Published by Wiley-VCH GmbH

the perovskite film. However, after changing the sampled area on the MAPI surface, it turned out that the water itself did not have such a destructive influence on the MAPI surface as shown by the long-lasting NAP-XPS characterization in the same perovskite sample spot. Namely, when the investigation spot after the whole experiment with water vapor was changed to a fresh one ($UHV_{end\ fresh\ spot}$ in Figure 1), the collected NAP-XPS spectra showed that these changes are much smaller. To highlight the differences between regions that were as-prepared, exposed to 1 mbar of water vapor, and a new spot of the possibly "degraded" MAPI film from Figure 1, the collected NAP-XPS spectra are shown separately in Figure S1 in the Supporting Information. From the comparison, it can be seen that even when the MAPI film was previously exposed to water for 9.5 h the NAP-XPS spectra collected on a new, non-irradiated spot of the same sample do not significantly differ from the spectra taken on the as-prepared MAPI film. It is known that perovskites are supposedly able to hydrate in the presence of water and dehydrate to mono- and dihydrated adducts before irreversible degradation after applying UHV conditions again.[25] Our NAP-XPS spectra collected on the same MAPI spot after pumping down the system back to UHV (UHV_{end}) conditions showed that this is not the case in the presence of X-rays. Exposing the MAPI film simultaneously to water and X-rays caused irreversible degradation, which is in agreement with Ref. [11]. However, when the MAPI film was investigated in a new sample spot after switching off the water source and pumping down the system to UHV ($UHV_{end\ fresh\ spot}$ in Figure 1), we were still able to observe a small peak at higher BE ($\approx$535 eV) in the O 1*s* spectrum that could be related to possible hydration of the MAPI surface. Therefore, based on our results, we assume that as the X-rays are a source of energy and heat, they can catalyze reactions occurring on the MAPI surface with water. Thus, dehydration to mono- and dihydrated adducts before irreversible degradation after applying UHV conditions again is not possible anymore. In other words, it may be that a surface chemical reaction, that is, the reaction of water with the perovskite surface, is just slower without X-rays.

To check the influence of the photon flux on the degradation rate of the MAPI film in the presence of 1 mbar of water, in the next step, an investigation of possible beam damage of the MAPI film was carried on utilizing synchrotron-based NAP-XPS. The corresponding NAP-XPS spectra of the C 1*s* (a, f), N 1*s* (b, g), Pb 4*f* (c, h), I 4*d* (d, i), and VB (e, j) collected in situ under 1 mbar of water vapor using excitation energy of 520 eV and two photon fluxes of 9.92×10^{11} photon s^{-1} (higher) and 7.44×10^{11} photon s^{-1} (lower, by detuning the undulator) are shown in Figure 2. The top panel in Figure 2 shows the evolution of the NAP-XPS spectra collected with the higher (9.92×10^{11} photon s^{-1}) and the bottom panel with the lower (7.44×10^{11} photon s^{-1}) photon flux. The peak positions in the NAP-XPS spectra collected on the as-prepared sample (time = 0 min, topmost spectrum) agree with the data shown in Figure 1. The synchrotron-based NAP-XPS characterization of the MAPI film in the presence of 1 mbar of water was done with 4.5 min intervals in Figure 2. It can be seen that the X-rays caused decomposition of the perovskite; its rate strongly depends on the used photon flux. The higher the photon flux, the faster the degradation. Under X-ray illumination and in the presence of 1 mbar of water, the bond between carbon and nitrogen in methylammonium is broken, and NH_3 is created. This is deduced from the observed decrease of the peak at 286.6 eV in the C 1*s* spectra and the peak at 402.6 eV in N 1*s* spectra as well as the appearance of a new peak at 400.5 eV[20] in the N 1*s* spectra in Figures 2a,f and 2b,g. However, the MAPI film is not completely decomposed. The peaks related to the CH_3NH_3 are still visible in the NAP-XPS spectra collected 1 h after starting the experiment. Besides that, in the Pb 4*f* and I 4*d* spectra we detected a shift of the peaks' binding energies of about −0.8 eV accompanied by the same change in VBM. Approximately, while the changes for the higher photon flux were noticed about 25 min after starting the measurements, for the lower photon flux, those changes were observed only after 45 min. Exposing the MAPI film to a combination of synchrotron-based X-rays and water vapor also produced the appearance of a peak at 136.8 eV in the Pb 4*f* spectra, which is typically attributed to the formation of "metallic lead"[22,26] in the MAPI crystal. After the time needed for the main changes in the NAP-XPS spectra to occur (Figure 2) a small (−0.1 eV) BE shift towards lower binding energy was observed.

The changes in the relative ratios of carbon (a), nitrogen (b), lead (c), and iodine (d) in the perovskite surface region are displayed in Figure 3. These values were extracted from the measurements done with excitation energy of 520 eV and using two different photon fluxes in the presence of 1 mbar of water vapor (i.e., from the analysis of the NAP-XPS results presented in Figure 2). As can be seen, initially there is a decrease of carbon and nitrogen and an increase of lead and iodine at the perovskite surface for both photon fluxes. However, as the MAPI film is further exposed to X-rays and water, for the higher photon flux, an increase of carbon, constant nitrogen, and decrease of lead and iodine relative concentrations are observed. In the case of the lower photon flux, the observation is similar, but the changes are propagating with a lower rate.

In Figure 4, the evolution of the MAPI surface depending on different environmental treatments was investigated using FESEM. Data is shown for fields of view of $2\times2\ \mu m^2$. The as-prepared MAPI film, grown on the FTO substrate, shows highly oriented large grains (Figure 4a). Exposing this film to the monochromatized X-ray beam (from the laboratory-based NAP-XPS instrument) with the energy of 1486.6 eV for 4 h (Figure 4b) produces some holes between the MAPI grains. In a few places, the accumulation of small islands is visible. However, exposing the MAPI film to 1 mbar of water vapor for 5 min (Figure 4c) or to 1 mbar of a mixture of water vapor and oxygen gas for 1 h (Figure 4d) does not cause such changes. The most significant changes in the MAPI morphology occurred when it was exposed to the synchrotron radiation beam (Figure 4e).

In the next step, we prepared MAPI-based solar cells in an n–i–p device architecture similar to Ref. [27] comprising glass/ITO/SnO_2/MAPI/spiDOT/Au, where ITO is indium-doped tin oxide and spiDOT is a 60:40 wt% mixture of 2,2′,7,7′-tetrakis (*N*,*N*-di-*p*-methoxyphenylamine)-9,9′-spirobifluorene (spiro-OMeTAD) and water-free poly(3,4-ethylenedioxythiophene) (PE-

© 2020 The Authors. Published by Wiley-VCH GmbH

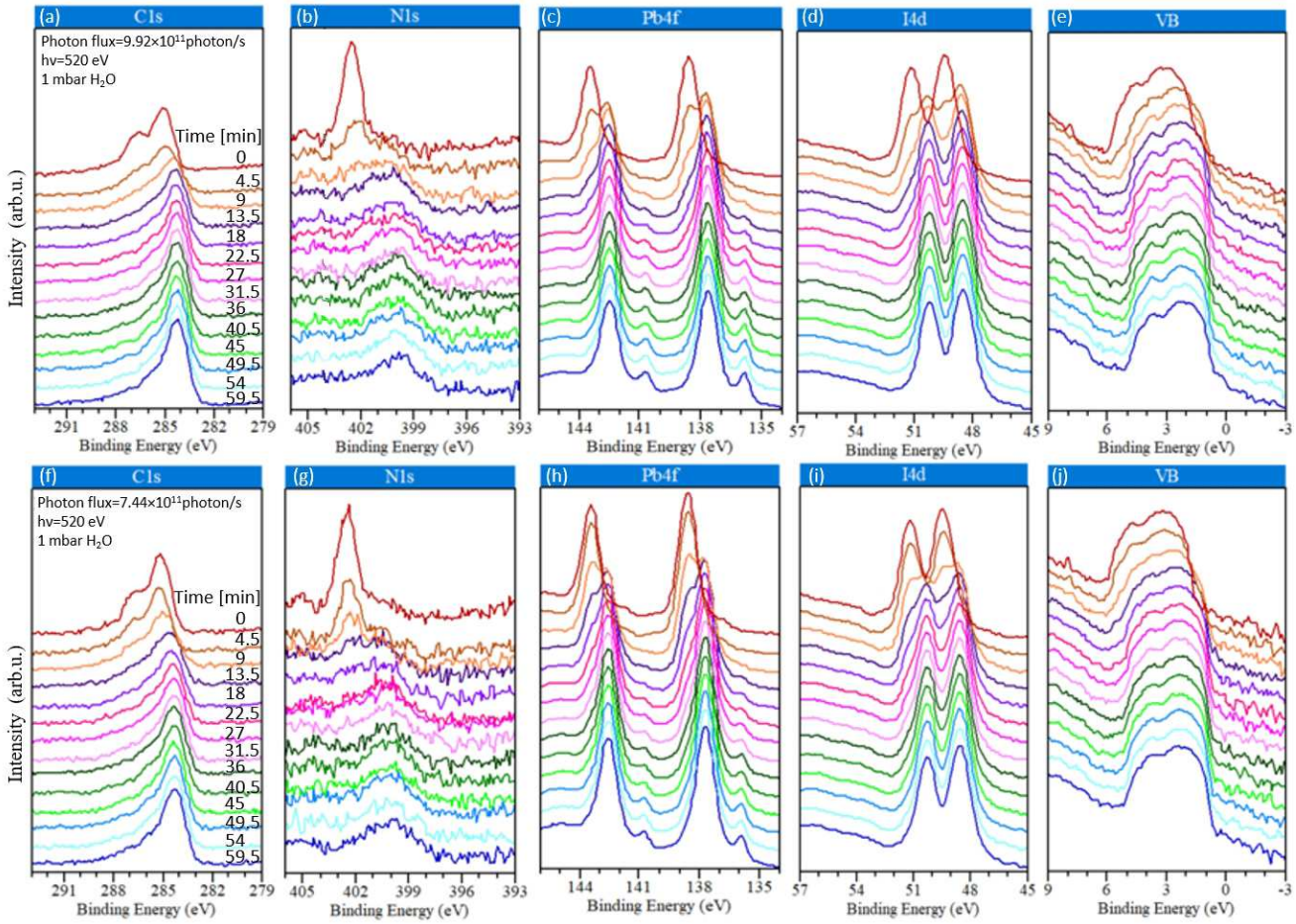

Figure 2. Exposure of $CH_3NH_3PbI_3$ film to 1 mbar of water and two different synchrotron-based X-ray fluxes using an excitation energy of 520 eV in a cycling mode: C 1*s* (a, f), N 1*s* (b, g), Pb 4*f* (c, h), I 4*d* (d, i), VB (e, j). Top panel: Higher photon flux of 9.92×10^{11} photon s^{-1} (4.05 sun); bottom panel: lower photon flux of 7.44×10^{11} photon s^{-1} (3.04 sun).

DOT). The MAPI absorber layer was prepared from DMF/DMSO solution via spin-coating.[28] Solar cells were investigated in a high-throughput ageing system according to the ISOS-L-1I protocol at open-circuit voltage (V_{OC}) to provide similar operating conditions as during the NAP-XPS studies. A constant illumination of 1, 0.5, and 0.32 suns including UV light, was used; the cells were kept at 25 °C in N_2 atmosphere. *J–V* scans for every sunlight dose were collected on 3–5 cells each in an interval of 3 h over 600 h in total. All parameters [PCE, fill factor (FF), short-circuit current density (J_{SC}), V_{OC}] in Figure 5a–d are normalized to the initial values. The long-term stability test has shown that all parameters are affected by the photon dose. Slower performance degradation for lower illumination intensity is distinguishable. Especially the initial "burn-in" efficiency loss is less pronounced for reduced illumination intensity. While having started at comparable efficiencies, after 600 h of illumination, samples receiving the lowest photon flux thus yield the highest PCE, V_{OC}, and FF values of the tested devices (tabulated values can be found in Figure S2).

3. Discussion

Degradation of the MAPI film under different environmental conditions was extensively studied by researchers in the past years.[8–10,14–16] It has been reported that many sources cause the PSC's performance to decrease over time. Heat, humidity, exposure to visible and UV light, migration of gold metal from the contacts into the absorber layer, or migration of other species into or out of the absorber layer were suggested.[8–13] Also, depending on the degradation source, different degradation paths have been proposed. However, reports significantly differ in the observed extent of solar cell degradation following exposure to the same medium, like, for example, water, with consequences ranging from very fast[29] to negligible[30] decomposition. The discrepancy in the degradation rates for the same medium can partially be related to the used characterization conditions, different preparation techniques, precursors, device designs, and others. Das et al.[31] have investigated MAPI films under open-circuit and applied potential, both in the dark and under illumination, and have found that the degradation paths and their respective rates strongly depend on the used

© 2020 The Authors. Published by Wiley-VCH GmbH

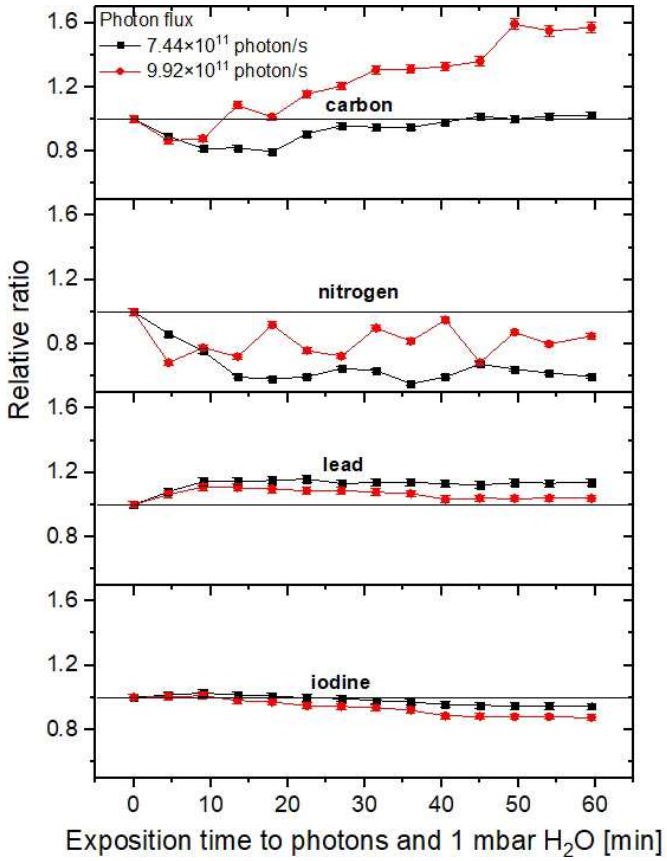

Figure 3. Relative carbon (a), nitrogen (b), lead (c), and iodine (d) ratio in the $CH_3NH_3PbI_3$ film exposed to 1 mbar of H_2O and two photon fluxes of 9.92×10^{11} photon s^{-1} (higher, 4.05 sun), and 7.44×10^{11} photon s^{-1} (lower, 3.04 sun) versus measurement time.

experimental conditions. Namely, in the dark under open-circuit conditions, the MAPI film preserved its chemical composition. The chemical composition was also maintained when the MAPI film was investigated in the dark under an applied voltage. However, when the light was switched on under open-circuit conditions, the MAPI film quickly degraded. Therefore, it is highly like that light has a strong influence on the perovskite film stability.

In our work, we investigated the real-time changes in the MAPI perovskite composition and electronic structure under the influence of different photon fluxes and water vapor conditions using NAP-XPS technique (Figures 1 and 2). We have found that irradiation has a detrimental impact on the chemical and electronic properties of the MAPI film. To correlate the photon fluxes used during NAP-XPS characterization with the number of suns we performed calculations that are shown in Supporting Information. For laboratory-based NAP-XPS studies (Figure 1), we got 0.01 sun illumination, and for the research conducted on a synchrotron (Figure 2) with a smaller and larger photon fluxes of 3.04 and 4.05 suns, respectively. These values are therefore below and above the illumination used during our *J-V* characterization and may also explain the degree of changes observed in the NAP-XPS spectra and in the *J-V* characteristics, as discussed below.

In particular, when the MAPI film was investigated in the same spot in the presence of up to 1 mbar of water with the lowest photon flux [using laboratory-based X-rays source (Figure 1)] for a prolonged time the changes in the NAP-XPS spectra were minimal. Only a small intensity decrease of peaks related to the CH_3NH_3 in the C 1*s* and N 1*s* NAP-XPS spectra was observed that could suggest the partial release of MA from the MAPI crystal. Nonetheless, when the sampling spot on the MAPI film after exposure to water vapor and X-rays for hundreds of minutes was changed there were almost no changes detected in the NAP-XPS spectra. Also, no peak shifts appeared in the NAP-XPS spectra collected with the laboratory-based anode (Figure 1) that would indicate electronic changes in the MAPI film during exposure to water vapor and X-rays.

When the MAPI film was investigated in the same sample spot in the presence of 1 mbar of water vapor using synchrotron-based radiation (Figure 2) that offers a much higher photon flux, the changes in the NAP-XPS spectra of this film propagated with the investigation time. Namely, a decrease of the MA-related component in the C 1*s* and N 1*s* and the iodine signal in the I 4*d* (Figures 2 and 3) and the occurrence of a peak at 136.8 eV in the Pb 4*f* (Figure 2c,h) NAP-XPS spectra were observed.

The intensity decrease of the XPS peaks does not necessarily have to be related to a potential release of these components from the investigated film. As discussed in our previous work[26]

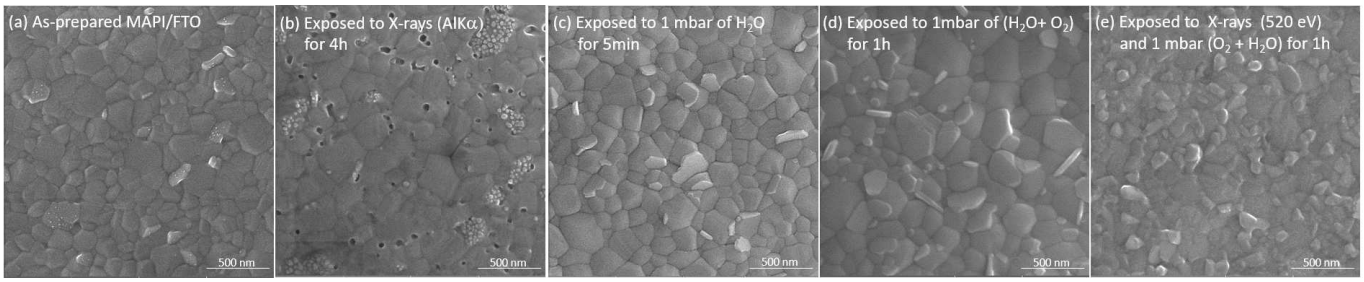

Figure 4. X-ray, water, and oxygen interaction with the $CH_3NH_3PbI_3$ film. Top-view FESEM images of the as prepared (a), exposed to the beam of Al K_α X-rays (photon flux of 6.1×10^9 photon s^{-1}, 0.01 sun) for 4 h (b), exposed to 1 mbar of water vapor for 5 minutes (c), exposed to 1 mbar of (0.5 H_2O + 0.5 O_2) for 1 h (d), exposed for 1 h to 1 mbar of (0.5 H_2O + 0.5 O_2) and X-ray beam with an excitation energy of 520 eV (photon flux = 9.92×10^{11} photon s^{-1}, 4.05 sun) (e) $CH_3NH_3PbI_3$/FTO/glass stack. The field of view is 2×2 μm^2 and the scale bar 500 nm.

© 2020 The Authors. Published by Wiley-VCH GmbH

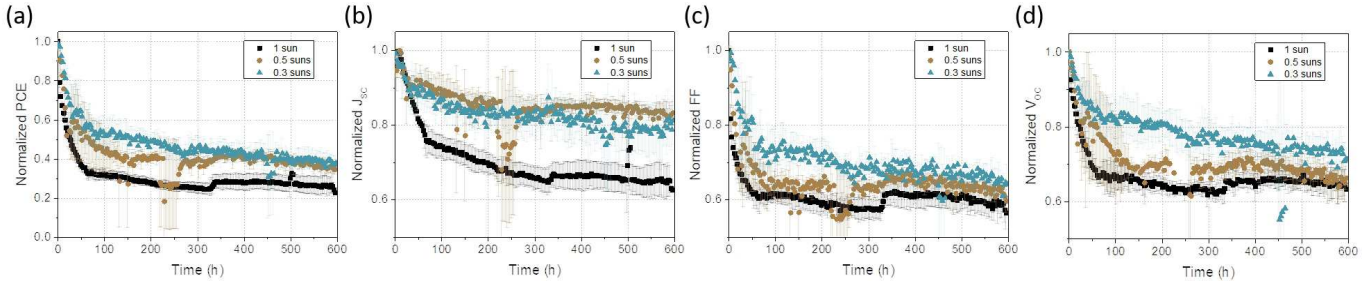

Figure 5. Normalized solar cell parameters: power conversion efficiency (PCE, a), short circuit current (J_{SC}, b), fill factor (FF, c) and open circuit potential (V_{OC}, d) from reverse current density-voltage scans over aging time using 1, 0.5 and 0.32 suns illumination, adjusted by the use of neutral density filters. Aging was performed at room temperature, in N_2, under UV/VIS/NIR illumination. During aging, the samples were kept at V_{OC} and measured every three hours.

we attribute this intensity decrease and the occurrence of "metallic lead" in the XPS spectra to the creation of Frenkel defects: methylammonium and iodine form interstitials in the ABX_3 perovskite crystal structure under irradiation by light or X-rays. In particular, Frenkel defects appear in an ionic solid that usually possesses a low coordination number or a considerable disparity in the sizes of ions. Therefore, it is highly possible to create such defects in the MAPI film, where there is a significant disparity in ion size. The remaining charges in the vacancy sites after the creation of Frenkel defects have an s-like orbital character that can readily hybridize with the neighboring valence states. Such hybridization, when it occurs, reduces the photoionization cross-section of elements and is observed as an intensity decrease of a specific core level (C 1*s*, N 1*s*, I 4*d*, etc.) in the XPS spectra. Moreover, the population swapping of Frenkel defects from the ionic state back to the metallic configuration promotes the charge redistribution to obtain a "physical metallic" state in terms of the charge balance between coexisting covalent and ionic subsystems.[26] Therefore, a reduction of a core level's intensity and the simultaneous occurrence of the "metallic lead" in the XPS spectra (Figure 2c,h) is a footprint of the creation of Frenkel pair defects, like MA^+ and I^- interstitials, in the MAPI film.[26]

Furthermore, binding energy shifts (Figure 2) were observed in the NAP-XPS spectra collected on the MAPI film using synchrotron radiation. We assume that this phenomenon could be either related to an insufficient charge extraction and grounding during prolonged measurement time using a highly brilliant X-ray source. In particular, during our synchrotron-based studies, we observed that the sample current during the NAP-XPS measurements increased over time. For example, during the data acquisition with excitation energy of 520 eV using higher photon flux the initial sample current of 10 μA increased after 3 min to 11.23 μA and after 30 min to 13.8 μA. Electronic changes due to the rearrangement of the atoms in the perovskite crystal are also possible. In the organo-metal-halide perovskite solar cells, both anions and cations tend to migrate inside the device and alter its electronic properties. Another possible explanation for the peak shifts in the NAP-XPS spectra could be related to the optical Kerr effect that creates a built-in electric field in the film. Namely, an intense beam of light in a solid can provide the modulating electric field, without the need for an external field to be applied, and is called optical Kerr or AC Kerr effect. This effect only becomes significant with very intense beams such as those from lasers, synchrotron radiation sources, or sunlight simulators. Further work needs to be done to fully understand the origin of the peak shifts in the NAP-XPS spectra collected on the MAPI film using synchrotron-based X-rays radiation, which is beyond the scope of this work.

The amount of water used in our studies had a negligible effect on the amount of destruction of the MAPI film. Still, it should be pointed out that water has a non-negligible impact on the damage of MAPI at higher concentrations.[6] As shown in Figure 1, even when the MAPI film was constantly exposed to water vapor for 570 min, the changes in its chemical or electronic structure were almost invisible in the NAP-XPS spectra (see also Figure S1). In our experiment, photons turned out to be the major devastating agent of this film. Also, our FESEM studies showed that the morphology of the perovskite sample underwent radical deformation when it was exposed to photons. The effect of water on the perovskite film morphology was rather negligible with the applied dose in our experiment.

Generation of Frenkel defects during *J–V* characterization under high-power irradiation is also likely. It can be related to the initial V_{OC} and FF losses commonly observed in the PSCs (Figure 5).[32] The non-radiative annihilation of excitons, as well as the non-radiative recombination of electrons and holes, was supposed to be the underlying mechanism of the anion Frenkel-defect creation in alkali halides. Therefore, a commonly known enhanced PSCs degradation[33] under V_{OC} as compared to the maximum power point or J_{SC} conditions may also be related to the increased presence of charge carriers and excited states[34] that lead to increased creation of Frenkel defects. In the literature, the fast initial decrease in efficiency has been reported to be reversible[35] and seems to be linked to slow halide vacancy migration.[36] Another argument for Frenkel pairs being a cause for the decline of the PCE during stability tests is their creation trend in time. In particular, at first, the number of Frenkel pairs (for alkali halides) increases with the irradiation time linearly, then sub-linearly, and finally reaches a saturation plateau.[37] This trend corresponds to the typical PCE decline trend during long-term stability tests, as also observed in our results shown in Figure 5. As the Frenkel defects can be self-

© 2020 The Authors. Published by Wiley-VCH GmbH

annihilated when the electric field is released,[38,39] and the efficiency of PSCs can be restored by resting the device in the dark, in air or N_2 at equilibrium,[36,40] the recovery process observed for these devices could also be attributed to the Frenkel defects' self-annihilation. Nonetheless, it was also reported that Frenkel defects cause hystereses[41] during *J-V* characterization. Such hystereses are also observed in our *J-V* characteristics (Figure S2), and they depend on the used illumination, that is, stronger illumination means larger hysteresis, which agrees with the proposed increased creation of Frenkel defects with higher photon flux. Moreover, our studies showed that initially similar PSCs efficiencies measured using 0.32, 0.5, and 1 suns, after longer ageing time, decreased the most for the highest photon flux used (1 sun, table in Figure S2).

Our recent studies[42] have shown that a very simple and cost-effective solution to reduce hysteresis during PSCs operation is to deposit an ultrathin aluminum oxide layer on top of the perovskite film using atomic layer deposition at room temperature.[6,9,22,42,43] The polaronic states of Al_2O_3 take up charge from the MAPI substrate. This charge is then transferred to and stabilized in the excitonic states of Al_2O_3.[22]

4. Conclusions

We conducted in situ near-ambient pressure X-ray photoelectron spectroscopy (NAP-XPS) studies to track the changes in the perovskite chemistry under different conditions in real-time. $CH_3NH_3PbI_3$ (MAPI) perovskite layers changed their chemical and electronic nature with time upon illumination. As the ex situ field emission scanning electron microscopy (FESEM) studies showed, not only the surface chemical composition but also the morphology of the MAPI films changed due to the lighting. The collected results have revealed that the observed changes in the NAP-XPS spectra are mainly caused by the X-ray beam. Exposure to 1 mbar of water vapor for a prolonged time had a negligible effect on the perovskite chemistry or morphology. Dependence of the perovskite decomposition rate on the number of photons incident on the sample was found. With more photons impinging on the MAPI surface, faster chemical and electronic, as well as morphological changes, occurred. The main observation from the NAP-XPS results is an initial reduction of carbon and nitrogen as well as an increase of lead and iodine signals accompanied by spectral shifts towards lower binding energies. The current density–voltage (*J–V*) characterization over 600 h using different illuminations (0.32, 0.5, and 1 suns) revealed that initially similar power conversion efficiency (PCE) values decrease with illumination time as a function of photon flux: The most robust PCE decrease is observed for the highest photon flux. By comparing our NAP-XPS results with the solar cell performance over time, we believe that the initial PCE decrease originates from the creation of Frenkel pair defects in the MAPI film under illumination. We assume that their creation under highly intense light might be much faster than the chemical reaction of water vapor with the perovskite and thus may explain the collected NAP-XPS results. As Frenkel defects can be self-annihilated when the light and voltage are turned off, we believe that the so-called "dark recovery" reported in the literature is caused by the self-annihilation of Frenkel defects in the perovskite crystal. Also, we have demonstrated that the number of Frenkel defects depends strongly on the photon flux. The higher the photon flux, the faster and higher is the creation of Frenkel defects, and thus the stronger is the degradation of PCE and the hysteresis in the *J–V* characteristics. Therefore, our results strongly suggest that to significantly extend the lifetime of PSCs a practical methodology to limit or even prohibit Frenkel defect creation under operation needs to be developed.

Experimental Section

Perovskite film and solar cell preparation: The MAPI absorber layer was prepared from DMF/DMSO solution with spin-coating according to our recipe published already in Ref. [28] The solar cells were prepared in an n-i-p similar to Ref. [24] The perovskite film was prepared on the ITO coated glass covered by a SnO_2 electron-transporting layer. As hole-transporting layers spiDOT were used. Gold was used as back contact. Layer thicknesses of the ITO/SnO_2/$MAPbI_3$/SpiDOT/Au stack amount to about 150, 40, 350, 100, and 80 nm, respectively.

NAP-XPS: The laboratory-based NAP-XPS studies were performed on the SPECS Surface Nano Analysis GmbH tool available at the Charles University in Prague (Czech Republic). More details about this instrument can be found elsewhere.[17,18] The base pressure in the analysis and in situ-load-lock chambers was in the range of 10^{-9} mbar. The "chamber-in-chamber" design allows the investigation of the perovskite film under different environmental conditions, that is, the perovskite film can be at the same time exposed to constant water vapor (at pressures ranging from 10^{-9} mbar up to 1 mbar) and investigated by XPS offering thus in situ studies of the perovskite chemical interaction with water. The XPS spectra were collected with an Al K_α anode (excitation energy of 1486.6 eV) at a photoelectron take-off angle of 90°. The flux of photons impinging on the perovskite film during XPS measurements was equal to 6.1×10^{9} photons s^{-1}, this was the lowest used in this work during NAP-XPS studies. The pressure during experiment was changed from 10^{-9} to 10^{-3}, 10^{-2}, 10^{-1}, and 1 mbar by introducing water vapor into the NAP cell chamber with the perovskite film. The perovskite film was investigated under UHV conditions (10^{-9} mbar) three times: in the same sample spot before and after water insertion into the NAP cell and the third time in a fresh spot of the same sample previously exposed to water. In order to check the influence of the photon flux on the degradation rate of the perovskite film under 1 mbar of water the MAPI film was investigated by means of synchrotron-based NAP-XPS. The synchrotron-based NAP-XPS studies were conducted at the CIRCE beamline at the ALBA Synchrotron Light Source in Spain, using the Phoibos NAP150 electron energy analyzer also from SPECS.[44] During this experiment, MAPI films were investigated in the presence of 1 mbar of water vapor using an excitation energy of 520 eV and two different photon fluxes of 9.92×10^{11} photon s^{-1} (highest used), and 7.44×10^{11} photon s^{-1} (middle used in this studies, by detuning the undulator). All spectra were calibrated with respect to the Pb $4f_{7/2}$ peak position at 138.6 eV. For relative ratio determination XPS spectra were fitted using CasaXPS. It should be noted that for the higher excitation energy of 1486.6 eV (using laboratory-based NAP-XPS tool) photoelectrons detected in given spectra carry information from areas deeper below the surface than those produced by synchrotron radiation using 520 eV radiation. Therefore, for the laboratory-based

© 2020 The Authors. Published by Wiley-VCH GmbH

NAP-XPS spectra, there is a mix of information from the "bulk" area and the surface region; thus, the changes may be less pronounced than for lower energy photons, regardless of the photon flux. However, it is proven in our experiment that using the same excitation energy of 520 eV and different photon flux there is a clear dependency of the perovskite degradation on the photon flux.

FESEM: The surface morphology of MAPI films exposed to different stresses (as-prepared, exposed to X-rays with different fluxes and energies, treated with water, and a mixture of water and oxygen) were examined using the FESEM Tescan Mira 3 available at the Charles University in Prague (Czech Republic). FESEM images were collected in the in-beam secondary electrons mode using an accelerating voltage of 30 kV, a working distance <3 mm with an electron beam spot size of 2 nm. The field of view of the presented results is $2\times2\ \mu m^2$, the scale bar is 500 nm.

Ageing of solar cells: Ageing was performed in a high-throughput ageing system[45] under V_{OC} load condition in order to provide similar operating conditions as during NAP-XPS studies. Cells were actively cooled to 25 °C in nitrogen atmosphere. Illumination was constant with 1, 0.5, and 0.32 suns, adjusted by the use of neutral density filters including UV light. For each sunlight dose, *J-V* scans were collected on 3–5 cells every 3 h over 600 h in total. *J-V* curves of the perovskite solar cells were scanned with a digital source meter (Keithley model 2400) in two consecutive sweeps without pre-biasing of the device, first in reverse direction from 1.2 to −0.1 V, and immediately afterwards in forward direction from −0.1 to 1.2 V. The scan rate was 100 mV s^{-1}. A metal-halide lamp with H2 filter was used, mimicking AM 1.5G spectra (see Figure S3). The illumination intensity was actively controlled with the help of a silicon irradiation-sensor, which itself was calibrated using a silicon reference cell from Fraunhofer ISE, adjusted to 100 mW cm^{-2}. By the overlap of orthogonal ITO and gold patterns, both 4 mm in width, the active area of 0.16 cm^2 was defined.

Acknowledgements

The CERIC-ERIC consortium is acknowledged for financial support under project numbers 20172012, 20172014, and 20177005. This work was also partially supported by the German Research Foundation (DFG, SCHM 745/31-1). The synchrotron-based NAP-XPS experiments were performed at the CIRCE beamline at ALBA Synchrotron with the collaboration of ALBA staff. Open access funding enabled and organized by Projekt DEAL.

Conflict of Interest

The authors declare no conflict of interest.

Keywords: field emission scanning electron microscopy · Frenkel defects · near-ambient pressure X-ray photoelectron spectroscopy · perovskite · photon-induced degradation

[1] H.-S. Kim, C.-R. Lee, J.-H. Im, K.-B. Lee, T. Moehl, A. Marchioro, S.-J. Moon, R. Humphry-Baker, J.-H. Yum, J. E. Moser, M. Grätzel, N. G. Park, *Sci. Rep.* **2012**, *2*, 591.
[2] M. M. Lee, J. Teuscher, T. Miyasaka, T. N. Murakami, H. J. Snaith, *Science* **2012**, *338*, 643.
[3] G. Hodes, *Science* **2013**, *342*, 317.
[4] K. Wojciechowski, M. Saliba, T. Leijtens, A. Abate, H. J. Snaith, *Energy Environ. Sci.* **2014**, *7*, 1142.
[5] T. Leijtens, G. E. Eperon, N. K. Noel, S. N. Habisreutinger, A. Petrozza, H. J. Snaith , *Adv. Energy Mater.* **2015**, *5*, 1500963.
[6] M. Kot, C. Das, Z. Wang, K. Henkel, Z. Rouissi, K. Wojciechowski, H. J. Snaith, D. Schmeisser, *ChemSusChem.* **2016**, *9*, 3401.
[7] Z. Wang, D. P. McMeekin, N. Sakai, S. van Reenen, K. Wojciechowski, J. B. Patel, M. B. Johnston, H. J. Snaith, *Adv. Mater.* **2017**, *29*, 1604186.
[8] T. A. Berhe, W.-N. Su, C.-H. Chen, C.-J. Pan, J.-H. Cheng, H.-M. Chen, M.-C. Tsai, L.-Y. Chen, A. Aregahegn Dubale, B.-J. Hwang, *Energy Environ. Sci.* **2016**, *9*, 323.
[9] M. Kot, L. Kegelmann, C. Das, P. Kus, N. Tsud, I. Matolinova, S. Albrecht, V. Matolin, D. Schmeisser, *ChemSusChem.* **2018**, *10*, 3640.
[10] D. Wang, M. Wright, N. K. Elumalai, A. Uddin , *Solar Energy Mater. Sol. Cells* **2016**, *147*, 255.
[11] F. Matsumoto, S. M. Vorpahl, J. Q. Banks, E. Sengupta, D. S. Ginger, *J. Phys. Chem. C* **2015**, *119(36)*, 20810.
[12] G. Murugadoss, S. Tanaka, G. Mizuta, S. Kanaya, H. Nishino, T. Umeyama, H. Imahori, S. Ito, *Jpn. J. Appl. Phys.* **2015**, *54(8)*, 08KF08.
[13] J. A. Christians, P. A. Miranda Herrera, P. V. Kamat, *J. Am. Chem. Soc.* **2015**, *137*, 1530–1538.
[14] R. Brenes, D. Guo, A. Osherov, N. K. Noel, C. Eames, E. M. Hutter, S. K. Pathak, F. Niroui, R. H. Friend, M. Saiful Islam, H. J. Snaith, V. R. Bulovic, T. J. Savenije, S. D. Stranks, *Joule* **2017**, *1*, 155.
[15] D. W. deQuilettes, W. Zhang, V. M. Burlakov, D. J. Graham, T. Leijtens, A. Osherov, V. Bulovic, H. J. Snaith, D. S. Ginger, S. D. Stranks, *Nat. Commun.* **2016**, *7*, 11683.
[16] Y. Tian, M. Peter, E. Unger, M. Abdellah, K. Zheng, T. Pullerits, A. Yartsev, V. Sundstrom, I. G. Scheblykin, *Phys. Chem. Chem. Phys.* **2015**. *17*, 24978–24987.
[17] M. Vorokhta, I. Khalakhan, M. Vondráček, D. Tomeček, M. Vorokhta, E. Marešová, J. Nováková, J. Vlček, P. Fitl, M. Novotný, P. Hozák, J. Lančok, M. Vrňata, I. Matolínová, V. Matolín, *Surf. Sci.* **2018**, *677*, 284–290.
[18] O. V. Larina, P. I. Kyriienko, D. Y. Balakin, M. Vorokhta, I. Khalakhan, Y. M. Nychiporuk, V. Matolín, S. O. Soloviev, S. M. Orlyk, *Catal. Sci. Technol.* **2019**, *9(15)*, 3964–3978.
[19] R.-P. Xu, Y.-Q. Li, T.-Y. Jin, Y.-Q. Liu, Q.-Y. Bao, C. O'Carroll, J.-X. Tang, *ACS Appl. Mater. Interfaces* **2018**, *10*, 6737–6746.
[20] X.-L. Zhou, F. Solymosi, P. M. Blass, K. C. Cannon, J. M. White, *Surf. Sci.* **1989**, *219*, 294.
[21] M. Kot, K. Wojciechowski, H. Snaith, D. Schmeißer, *Chem. Eur. J.* **2018**, *24*, 3539.
[22] M. Kot, K. Henkel, K. Müller, L. Kegelmann, S. Albrecht, N. Tsud, P. Kús, I. Matolinová, D. Schmeißer, *Energy Technol.* **2019**, *7*, 1900975.
[23] NIST. X-ray Photoelectron Spectroscopy Database https://srdata.nist.gov/xps/EnergyTypeValSrch.aspx (accessed April 20, 2020).
[24] M. M. Lee, J. Teuscher, T. Miyasaka, T. N. Murakami, H. J. Snaith, *Science* **2012**, *338*, 643.
[25] A. M. A. Leguy, Y. Hu, M. Campoy-Quiles, M. I. Alonso, O. J. Weber, P. Azarhoosh, M. van Schilfgaarde, M. T. Weller, T. Bein, J. Nelson, P. Docampo, P. R. F. Barnes, *Chem. Mater.* **2015**, *27(9)* 3397–3407.
[26] D. Schmeißer, K. Henkel, E. Pożarowska, L. Kegelmann, N. Tsud, M. Kot, *J. of Phys. Chem. C* **2019**, *123*, 23352–23360.
[27] L. Kegelmann, P. Tockhorn, C. M. Wolff, J. A. Márquez, S. Caicedo-Dávila, L. Korte, T. Unold, W. Lövenich, D. Neher, B. Rech, S. Albrecht, *ACS Appl. Mater. Interfaces* **2019**, *11(9)*, 9172–91811.
[28] N. Phung, R. Félix, D. Meggiolaro, A. Al-Ashouri, G. Sousa e Silva, C. Hartmann, J. Hidalgo, H. Köbler, E. Mosconi, B. Lai, R. Gunder, M. Li, K.-L. Wang, Z.-K. Wang, K. Nie, E. Handick, R. G. Wilks, J. A. Marquez, B. Rech, T. Unold, J.-P. Correa-Baena, S. Albrecht, F. De Angelis, M. Bär, A. Abate, *J. Am. Chem. Soc.* **2020**, *142*, 2364–2374.
[29] B. Conings, J. Drijkoningen, N. Gauquelin, A. Babayigit, J. D'Haen, L. D'Olieslaeger, A. Ethirajan, J. Verbeeck, J. Manca, E. Mosconi, F. De Angelis, H.-G. Boyen, *Adv. Energy Mater.*, **2015**, *5(15)*, 1500477.
[30] M. Kot, M. Vorokhta, Z. Wang, H. J. Snaith, D. Schmeißer, J. I. Flege, *Appl. Surf. Sci.* **2020**, *513*, 145596.
[31] C. Das, M. Wussler, T. Hellmann, T. Mayer, W. Jaegermann, *Phys. Chem. Chem. Phys.* **2018**, *20(25)*, 17180–17187.
[32] B. Chen, T. Li , Q. Dong, E. Mosconi, J. Song, Z. Chen, Y. Deng, Y. Liu, S. Ducharme , A. Gruverman, F. De Angelis, J. Huang, *Nat. Mater.* **2018**, *17*, 1020–1026.
[33] K. Domanski, E. A. Alharbi, A. Hagfeldt, M. Grätzel, W. Tress, *Nat. Energy* **2018**, *3*, 61–67.
[34] Y. Lin, B. Chen, Y. Fang, J. Zhao, C. Bao, Z. Yu, Y. Deng, P. N. Rudd, Y. Yan, Y. Yuan, J. Huang, *Nat. Commun.* **2018**, *9*, 4981.

© 2020 The Authors. Published by Wiley-VCH GmbH

[35] M. V. Khenkin, K. M. Anoop, I. Visoly-Fisher, S. Kolusheva, Y. Galagan, F. Di Giacomo, O. Vukovic, B. Ramesh Patil, G. Sherafatipour, V. Turkovic, H. G. Rubahn, M. Madsen, A. V. Mazanik, E. A. Katz , *ACS Appl. Energy Mater.* **2018**,*1*, 799–806.
[36] K. Domanski, B. Roose, T. Matsui, M. Saliba, S. H. T. Cruz, J.-P. C-Baena, C. R. Carmona, G. Richardson, J. M. Foster, F. De Angelis, J. M. Ball, A. Petrozza, N. Mine, M. K. Nazeeruddin, W. Tress, M. Gratzel, U. Steiner, A. Hagfeldt, A. Abate, *Energy Environ. Sci.* **2017**, *10*, 604–613.
[37] C. B. Lushchik in Condensed Matter Sciences, Vol. 13 (Ed.: R. A. Johnson, A. N. Orlov), Elsevier, Oxford, **1986**, pp. 473–475.
[38] H. Wei, J. Huang, *Nat. Commun.* **2019**, *10*, 1066.
[39] F. Lang, N. H. Nickel, J. Bundesmann, S. Seidel, A. Denker, S. Albrecht, V. V. Brus, J. Rappich, B. Rech, G. Landi, H. C. Neitzert, *Adv. Mater.* **2016**, *28*, 8726–8731.
[40] X. Tang, M. Brandl, B. May, I. Levchuk, Y. Hou, M. Richter, H. Chen, S. Chen, S. Kahmann, A. Osvet, F. Maier, H. P. Steinruck, R. Hock, G. J. Matt, C. J. Brabec, *J. Mater. Chem. A* **2016**, *4*, 15896.
[41] D.-Y. Son, S.-G. Kim, J.-Y. Seo, S.-H. Lee, H. Shin, D. Lee, N.-G. Park, *J. Am. Chem. Soc.* **2018**, *140*, 1358–1364.
[42] C. Das, M. Kot, T. Hellmann, C. Wittich, E. Mankel, I. Zimmermann, D. Schmeisser, M. K. Nazeeruddin, W. Jaegermann, *Cell Reports Physical Science* **2020**, *1*, 100112.
[43] M. Kot, C. Das, K. Henkel, K. Wojciechowski, H. J. Snaith, D. Schmeisser, *Nucl. Instrum. Methods Phys. Res. Sect. B* **2017**, *411*, 49–52.
[44] V. Pérez-Dieste, L. Aballe, S. Ferrer, J. Nicolas, C. Escudero, A. Milan, E. Pellegrin, *J. Phys. Conf. Ser.* **2013**, *425*, 072023.
[45] H. Köbler, S. Neubert, B. Glažar, M. Jankovec, M. Topič, B. Rech, A. Abate in *Proceedings of International Conference on Hybrid and Organic Photovoltaics (HOPV19) Roma, Italy, 2019 May 12th - 15th*, **2019.**

Manuscript received: June 20, 2020
Revised manuscript received: August 20, 2020
Accepted manuscript online: September 3, 2020
Version of record online: September 15, 2020

© 2020 The Authors. Published by Wiley-VCH GmbH